A Mechanically Robust Yet Highly Conductive Diblock Copolymer Solid Polymer Electrolyte for Ambient Temperature Battery Applications

*Andreas Bergfelt,[‡†] Guiomar Hernández,[‡] Ronnie Mogensen, Matthew J. Lacey, Jonas Mindemark, Daniel Brandell, Tim Melander Bowden**

Department of Chemistry – Ångström Laboratory, Uppsala University, Box 538, Lägerhyddsvägen 1, 751 21 Uppsala, Sweden

KEYWORDS: Block copolymer, solid polymer electrolyte, lithium ion battery, structural battery.

ABSTRACT: In this paper we present a solid polymer electrolyte (SPE) that uniquely combines ionic conductivity and mechanical robustness. This is achieved with a diblock copolymer poly(benzyl methacrylate)-poly(ε-caprolactone-r-trimethylene carbonate). The SPE with 16.7 wt% lithium bis(trifluoromethanesulfonyl)imide (LiTFSI) showed the highest ionic conductivity (9.1×10^{-6} S cm^{-1} at 30 °C) and apparent transference number (T_+) of 0.64 ± 0.04. Due to the employment of the benzyl methacrylate hard-block, this SPE is mechanically robust with a storage modulus (E') of 0.2 GPa below 40 °C, similar to polystyrene, thus making it a suitable material also for load-bearing constructions. The cell Li|SPE|$LiFePO_4$ is able to cycle

reliably at 30 °C for over 300 cycles. The promising mechanical properties, desired for compatibility with Li-metal, together with the fact that BCT is a highly reliable electrolyte material makes this SPE an excellent candidate for next-generation all-solid-state batteries.

INTRODUCTION

Solid polymer electrolytes (SPEs) are gaining research interest as replacements for flammable organic liquid electrolytes in lithium-ion battery devices owing to the strict safety standards employed in the electric automotive vehicles industry.[1-2] Furthermore, switching from a liquid electrolyte to an SPE introduces new design possibilities.[3-5] This applies to, for example, so-called 'structural batteries', where the battery is used as a construction material itself.[6] These have so far been dominated by liquid electrolytes, which render problems with leakage and the electrochemical stability and transfer the loadbearing function to primarily the electrodes and packaging materials. Currently, solid polymer electrolytes have sufficient mechanical integrity to prevent leakage and withstand bending strains, but their modulus is in the range of MPa. For applications where mechanical properties are important, SPEs should have a stiffness around 2–3 orders of magnitude higher.[7] If a mechanically robust solid electrolyte could be found this would generate a dramatic increase in structural design as well as flexibility. The ultimate aim of this field of research is to develop an SPE that combines high ionic conductivity, a high lithium ion transference number, electrochemical stability, and excellent mechanical properties to produce batteries with no restrictions on performance or design. However, experience has shown that these criteria are, to some degree, mutually exclusive. For example, when the mechanical

properties of an SPE are improved its ionic conductivity is generally decreased as both properties are correlated to the segmental motion of the polymer chains, but in opposing directions.[4, 8]

Several approaches have been used to address this problem. An increase in battery operating temperature typically improves ionic conductivity, but has a negative effect on mechanical properties.[9] Furthermore, with increasing operating temperature, parasitic reactions occur more readily, negatively affecting battery health and lifetime.[10] A potentially viable strategy for addressing this issue is to decouple the ionic conduction and mechanical properties of an SPE. This could possibly be achieved using block copolymers, with the working hypothesis that one block would confer mechanical strength to the SPE while the other would conduct ions.[5, 11-16] Since the blocks are chemically bonded to each other they behave macroscopically as a single material, but on a microscopic scale behave as two materials, each retaining its unique properties. To date, most of the research in this field has been focused on the polystyrene-polyethylene oxide (PS-PEO) block copolymer system.[17] The soft PEO block, however, displays inferior properties in terms of high crystallinity, low cation transference number and insufficient room temperature conductivity, which stimulates an ongoing search for alternatives. As the field of SPEs is growing, several exciting chemistries for both the soft and hard blocks are being developed, which is broadening the field.

Recent research efforts have highlighted alternative SPE materials based on polycarbonates and polyesters.[18] Materials such as poly(ethylene carbonate) (PEC) and poly(trimethylene carbonate) (PTMC) combine facile and non-exotic preparation with excellent ionic conductivity and high lithium-ion transference numbers.[19-21] Of particular interest are copolymers of poly(ε-caprolactone) (PCL) and poly(trimethylene carbonate) (PTMC).[19, 22-23] When the PCL to PTMC monomer ratio is 80:20 (80:20 PCL–PTMC), an ionic conductivity in excess of

10^{-5} S cm^{-1} was achieved at room temperature with a salt loading of 36 wt% lithium bis(trifluoromethanesulfonyl)imide (LiTFSI), making it possible to cycle half-cells at ambient temperature with good capacity.[24] The remarkable ion transport properties of this material, however, come at a penalty regarding the mechanical properties. Since amorphous, low-T_g materials like the PCL–PTMC copolymers are not mechanically stabilized by other means than molecular entanglements, they essentially behave as viscous liquids at the molecular level.[25] Macroscopically, this means that even at high molecular weights these materials are soft and sticky with insufficient mechanical properties for structural applications and making them vulnerable to dendrite formation during cycling which could short circuit the battery device during long-term usage.[26-27] Mechanical stabilization of this material using gamma irradiation to crosslink the electrolyte has been demonstrated, although with only a small improvement in mechanical properties.[25]

To improve the mechanical properties of SPEs, polystyrene[17] and poly(alkyl methacrylate)s[28] blocks have been widely investigated for block copolymer electrolytes. The PCL–PTMC platform, in turn, has also been employed as a soft block in such electrolytes, using polystyrene as the hard block, but with detrimental effects on the ionic conductivity.[29] To achieve a better conductive yet robust material, these two properties should be decoupled.[5, 28] For the hard blocks, acrylate- and methacrylate-based polymers are likely important candidates due to their wide availability, low toxicity and good electrochemical stability.[30] Poly(benzyl methacrylate) (PBnMA) is in this context an interesting and underutilized material for SPEs. The rate of polymerization of benzyl methacrylate (BnMA) is significantly faster than that of styrene, thus generating higher conversions in short reaction times.[31] The (PBnMA) block is also more electrochemically stable than poly(methyl methacrylate) (PMMA).[32]

Here, we thus present a block copolymer approach that combines the excellent ion transport properties of the PCL–PTMC copolymer with the robust mechanical properties of a second, stabilizing, poly(benzyl methacrylate) (PBnMA) block. This combination leads to outstanding Li^+ transport properties for an extremely robust electrolyte able to be used in load-bearing applications.

EXPERIMENTAL SECTION

Materials. Benzyl methacrylate (BnMA), *N,N,N′,N′′,N′′′*-pentamethylenetriamine (PMDETA), 2-hydroxyethyl 2-bromoisobutyrate, $CuBr_2$, stannous 2-ethylhexanoate, Al_2O_3 (Brockmann l, activated, basic). Other chemicals used included ε-caprolactone (Sigma Aldrich) and trimethylene carbonate (Boehringer Ingelheim). ε-Caprolactone was dried with CuH_2 overnight before being distilled and transferred to an argon-filled glove box. Solvents were used without further purification. LiTFSI (Purolyte, Ferro Corporation) was dried at 120 °C for 24 h before use. Lithium iron phosphate (LFP, Phostech Lithium), super P carbon black (Erachem), poly(vinylidene fluoride) (PVdF, Kynarflex 2801-00, Arkema), poly(ethylene oxide) (PEO, 4 000 000 g mol^{-1}, BDH Chemicals), and aluminum and copper foils were used as received. Poly(ε-caprolactone-*r*-trimethylene carbonate) (80:20 PCL–PTMC) PCL–PTMC copolymer with molar ratio 80:20 was synthesized as described in the literature.[19]

Poly(benzyl methacrylate) macroinitiator (PBnMA) synthesis. Benzyl methacrylate (BnMA) was filtered through 10 mL basic Al_2O_3 to remove the inhibitor before polymerization. The monomer (40 mL, BnMA), initiator (0.1 mL, EBiB-OH), ligand (0.1 μL, PMDETA) and catalyst (0.3 mg, $CuBr_2$) were placed in a Schlenk flask. Oxygen was removed over three freeze–

pump–thaw cycles using liquid nitrogen cooling. The flask was back-filled with argon and finally 20 mg CuBr was added to start the reaction. The reaction was performed in an oil bath set at 30 °C. The reaction was quenched after 3 h with 20 mL acetone, and the mixture was quickly filtered through basic Al_2O_3 into 400 mL ethanol to precipitate the polymer. The polymer was recovered through filtration and dried in a vacuum oven at room temperature. M_n (GPC): 25 583 g mol^{-1}, PDI: 1.13.

Poly(benzyl methacrylate)-b-poly(ε-caprolactone-r-trimethylene carbonate) (BCT) synthesis. The poly(benzyl methacrylate) macroinitiator (1 g) was transferred into an argon-filled glove box and mixed with 1 g dry toluene in a pre-dried 20 mL vial. After the macroinitiator was dissolved, 3.4 g ε-caprolactone, 0.57 g trimethylene carbonate, and 24 µL stannous 2-ethylhexanoate (1 M in toluene) were added. The vial was capped and transferred to a heating block and polymerize, at 130 °C for 24 h. The vial was removed from the heating block and ca. 10 mL THF was added to dissolve the polymer. The solution was precipitated into 400 mL of methanol. The polymer was collected via filtration and dried in a vacuum oven at room temperature. M_n (GPC): 79 000 g mol^{-1}, PDI: 2.0.

Poly(trimethylene carbonate) (PTMC) binder synthesis. 3 g of trimethylene carbonate was added to a pre-dried vial together with 9 g of dry toluene. Tin(II) 2-ethylhexanoate (1 M in toluene) (29.4 µL) was used as catalyst and 1-propanol (1 µL) as initiator. The reaction was allowed to polymerize at 120 °C for 24 h before being precipitated into a beaker of methanol. The polymer was dried in a vacuum oven. M_n (GPC): 10 000 g mol^{-1}, PDI: 1.95.

Gel permeation chromatography (GPC). The GPC system was an Agilent 1260 Infinity fitted with PolyPore columns and a refractive index detector. The mobile phase was THF

(1 mL min^{-1}) and the separation was performed at 35 °C. PMMA standards were used to calibrate the system.

Nuclear magnetic resonance (NMR). ^{1}H NMR spectra were recorded in $CDCl_3$ on JEOL Eclipse+ 400 MHz NMR spectrometer.

Electrolyte film preparation. The polymers were mixed with dry THF and LiTFSI (ca. 100 mg of polymer and 2 mL THF with a corresponding amount of LiTFSI). The films were cast in Teflon molds (20 mm in diameter) and the solvent was removed via controlled evaporation in a vacuum oven; the pressure was reduced to full vacuum (< 1 mbar) over 20 h before heating at 60 °C at full vacuum for 40 h. The resulting films were ca. 0.2 mm in thickness. All procedures were performed in an argon-filled glove box.

Differential scanning calorimetry (DSC). A TA instruments DSC Q2000 was used. The samples were hermetically sealed in aluminum pans in an argon-filled glove box. A −80 to 180 °C cooling/heating/cooling/heating cycle was used with a ramping speed of 10 °C min^{-1} for all the steps under a flow of N_2. The second heating ramp was used for measurement.

Small-angle neutron scattering (SANS). Data were obtained on the LOQ small-angle diffractometer at the ISIS Pulsed Neutron Source (STFC Rutherford Appleton Laboratory, Didcot, UK).[33] This is a fixed-geometry "white beam" time-of-flight instrument that utilizes neutrons with wavelengths between 0.2 and 1 nm. Data are simultaneously recorded on two two-dimensional, position-sensitive neutron detectors to provide a simultaneous Q range of 0.08–16 nm^{-1}. Once data of acceptable statistical precision had been accumulated, each raw scattering data set was corrected for the detector efficiencies, sample transmission, and background scattering, and converted to scattering cross-section data ($\partial\Sigma/\partial\Omega$ *vs.* Q) using the Mantid framework.[34] Samples were wrapped in thin aluminum foil and fixed with amorphous quartz

discs in aluminum holders. The aluminum holders were then mounted in a brass sample rack on a computer-controlled sample changer. In this configuration, the sample rack was thermostated using an electrical cartridge heater. The incident neutron beam was 11 mm in diameter, the moderator–sample distance was 10.980 m, and the sample-detector distance was 4.170 m. Each sample was typically measured for ca. 30 min at each temperature point.

Rheology. Rheology measurements were performed on a Discovery Hybrid Rheometer (DHR-2, TA Instruments) using an 8 mm parallel plate geometry at a controlled strain of 0.1% with an axial force of 5 N ± 0.5 N. The measurements were performed in ambient air.

Dynamical mechanical analysis (DMA). A DHR-2 (TA Instruments) with ETC was used in DMA tensile mode using film clamps. The measurements were performed using a strain factor of 100, at 1 Hz and 0.05 in displacement, and heating at 1 °C min^{-1}. The measurements were performed with dry N_2.

Electrochemical impedance spectroscopy (EIS). The ionic conductivity was measured using impedance spectroscopy with an SI 1260 Impedance Gain-Phase Analyzer (Schlumberger) at a frequency range of 1 Hz to 10 MHz with the amplitude set to 10 mV. The electrolytes were sandwiched between stainless steel electrodes in coin cells that were heated to 90 °C and cooled to anneal the electrolyte with the electrode surfaces before the measurements were carried out from 30 to 90 °C. The samples were equilibrated at every temperature for ca. 20 min before a new recording was performed. The resistance was evaluated with ZView (Scribner Associates) using a modified Debye equivalent circuit.[22]

Cyclic voltammetry. Cyclic voltammetry analysis was carried out on a VMP2 (Bio-Logic). A 20 mm disc of BCT17 electrolyte was sandwiched between a 14 mm lithium disc and an 18 mm stainless steel disc before being sealed in a laminated pouch bag. All procedures were carried out

in an argon-filled glove box. The pouch bag was annealed at OCV for 12 h at 60 °C before cycling was performed at 1 mV s^{-1}.

Transference number. Transference number measurements were performed on an SP-240 (Bio-Logic) connected to an oven operated at 60 °C. The cell was fabricated using 20 mm diameter BCT17 discs and two 16 mm diameter lithium electrodes. The stack was sealed in a laminated pouch bag using and was annealed at OCV for 24 h before measuring the impedance spectrum. After the impedance step, the cell was rested for 1 h before applying a voltage step of 20 mV and recording the current versus time. After 60 h, the impedance spectrum was measured again. The impedance data was fitted with ZView and the first current value recorded was considered as the initial current. The apparent transference number value was reported with 95% confidence limits using a code in R (see Supporting Information).

Battery cell preparation and cycling. For the symmetric Li │BCT17│Li cells, the BCT17 electrolyte (120 μm thickness and 12 mm diameter) was sandwiched between lithium electrodes (10 mm diameter) in coin cells. The cells were annealed at 55 °C for 3 h and then polarized for 4 h at 0.013 mA cm^{-2} current density with 90 min rest between plating and striping cycles at 30 and 55 °C. $LiFePO_4$ electrodes were prepared with a mixture of 75 wt% active material, 10 wt% carbon black, and 15 wt% binder (PVdF, BCT17, PTMC17) on aluminum foil. The slurry was prepared using *N*-methyl-2-pyrrolidone as solvent for the PVdF binder and tetrahydrofuran for the polymer electrolyte binders. The electrodes were transferred into a glovebox and dried at 120 °C for 12 h before cell preparation. The final electrodes presented 3 mg cm^{-2} mass loading. The electrolytes were cast directly onto the cathodes and vacuum-dried for 20 h before heating at 60 °C and full vacuum for 40 h before being assembled with lithium anodes and sealed in laminated pouch bags. Galvanostatic cycling was carried out on a Digatron MBT battery test

system at 30 and 60 °C between 2.7 and 4.2 V *vs.* Li^+/Li. Two-electrode experiments using the intermittent current interruption technique were performed on an MPG2 (Bio-Logic) at 60 °C. Current interruptions were made for 1 s at 5 min intervals following the analysis procedure reported by Lacey.[35]

RESULTS AND DISCUSSION

Polymer synthesis. The major challenge in polymer electrolyte research is to resolve the limitation imposed by the coupling of ion transport to polymer segmental motions which dictates that fast ion transport comes at a penalty of deteriorating mechanical properties. To enable battery electrolytes with useful mechanical properties, this dependence needs to be broken, which can be achieved by separating the load-bearing and ion-transporting functions to different parts of a microphase separated block copolymer. To this end, we have introduced a hard, high-T_g PBnMA block to the soft, low-T_g PCL–PTMC copolymer. This poly(benzyl methacrylate)-b-poly(ε-caprolactone-r-trimethylene carbonate) copolymer, here termed BCT, was synthesized in two steps, as outlined in Scheme 1, starting with the synthesis of a 26 000 g mol^{-1} PBnMA macroinitiator through atom transfer radical polymerization (ATRP). Gel permeation chromatography (GPC) analysis presented a monomodal peak with a low polydispersity index (PDI) of 1.13, indicating a well-controlled synthesis. Through the use of the ATRP initiator 2-hydroxyethyl 2-bromoisobutyrate a hydroxyl end-group was retained at the α-end to serve as an initiator for the ring-opening polymerization step to form the ion-conducting PCL–PTMC block. The resulting polymer was hard and white with a molecular weight of 79 000 g mol^{-1} according to GPC, corresponding to a degree of polymerization of 145 for the PBnMA block and

470 for the PCL–PTMC block. The GPC trace was broad but monomodal, indicating successful initiation by the macroinitiator, but with limited control since the PDI value reached as high as 2.0. ^{1}H-NMR (Figure S1) analysis revealed that the composition of the BCT polymer was 17 mol% PBnMA, 76 mol% ε-caprolactone, and 7 mol% trimethylene carbonate. The theoretical composition was set to 13.8 mol% PBnMA, 72.6 mol% ε-caprolactone, and 13.6 mol% trimethylene carbonate, representing a ε-caprolactone to trimethylene carbonate molar ratio 8.4:1.6.

Scheme 1. Reaction scheme for the synthesis of the poly(benzyl methacrylate)-poly(ε-caprolactone-*r*-trimethylene carbonate) (BCT) block copolymer. The first reaction utilizes atom transfer radical polymerization, and the second step utilizes ring-opening polymerization.

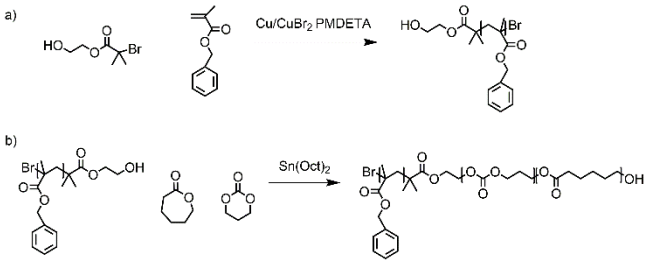

Thermal properties. The synthesized BCT copolymer was combined with LiTFSI salt and polymer electrolytes were prepared using solvent casting. The resulting electrolyte films did not exhibit the stickiness typical of soft, amorphous polymer electrolytes and they were notably mechanically stable, making them easy to handle. These samples are hereafter denoted BCT##, where the number ## is the weight percentage of LiTFSI in the electrolyte.

Differential scanning calorimetry (DSC) measurements revealed that the LiTFSI-free polymer (BCT0) was semi-crystalline, as shown in Table 1 and Figure S2. Considering that the PBnMA block is atactic and that the melting point is slightly below that of pure PCL (~60 °C), this is likely to arise from the crystallization of caprolactone repeating units. In addition, when adding LiTFSI, the degree of crystallinity decreased (Figure S2), as ion coordination of the ester groups in the caprolactone repeating units interferes with crystallization. When the content of LiTFSI was more than 9 wt% the electrolytes became completely amorphous, see Figure S2 for the DSC traces and Table 1 for the data from the second heat scan. The analysis also shows the lack of a distinctive second T_g, indicating that there is no clear phase separation in the BCT electrolytes based on the DSC data.

Table 1. DSC data for the BCT series with different amounts of LiTFSI, compared to 80:20 PCL–PTMC and PEO.

Entry	LiTFSI [wt%]	LiTFSI based on the conducting block [wt%]	T_g [°C]	T_m [°C]	T_c [°C]
BCT0	0	0	−42.3	49.7	1.8
BCT9	9.1	11.4	−41.0	44.4	−6.1
BCT17	16.7	20.9	−48.9	-	-
BCT23	23.1	28.9	−41.3	-	-
BCT29	28.6	35.8	−35.1	-	-
80:20 PCL–	28.0	28.0	−31.8	-	-

PTMC					
PEO	24.6	24.6	−34.0	32.5	61.6

Mechanical properties. The mechanical properties of the electrolyte are essential in a battery to allow for load-bearing functionalities. The immediately striking feature of the BCT copolymer is its rigidity – despite that it is predominantly made up of the soft PCL–PTMC copolymer. Moreover, this rigidity was retained when mixed with LiTFSI salt to form free standing polymer electrolyte films that are easy to handle (Figure S3).

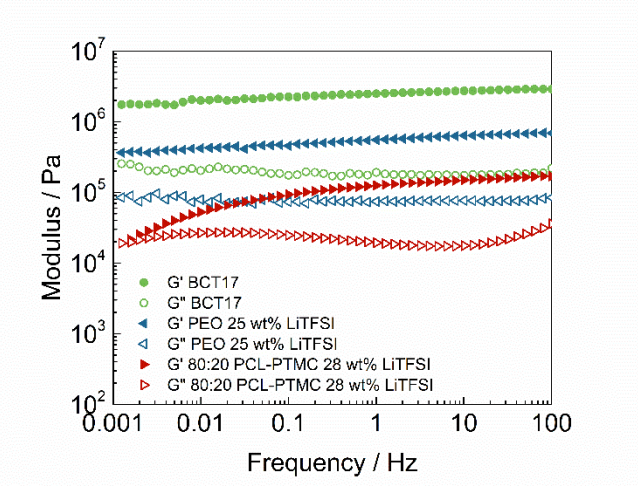

Figure 1. Oscillation frequency sweeps at 25 °C for BCT17, PEO (M_w of 4 000 000 g mol^{-1} and an ethylene oxide to LiTFSI ratio of 20:1 (24.6 wt% LiTFSI)) and 80:20 PCL–PTMC electrolyte (M_w 280 000 g mol^{-1}, PDI 2.02 and 28 wt% LiTFSI). Storage modulus G' and loss modulus G''.

The viscoelastic properties of BCT17 were investigated through oscillatory rheology and compared to an 80:20 PCL–PTMC copolymer with 28 wt% LiTFSI and a conventional PEO-

based electrolyte with a 20:1 EO:Li^+ ratio (24.6 wt% LiTFSI) (Figure 1). At 25 °C, the storage modulus G' is highest for BCT17. For both BCT17 and the PEO electrolyte, G' shows only limited frequency dependence, and G' > G'' (loss modulus) throughout the measured frequency range. In contrast, the 80:20 PCL–PTMC electrolyte shows marked frequency dependence for G', with a crossover point for G' and G'' at low frequencies. The lack of such a crossover point for BCT17 indicates that its viscous behavior will never be dominant and that the electrolyte will be dimensionally stable over time. In order to evaluate the mechanical properties as a function of temperature, dynamic mechanical analysis was performed on BCT17. As seen in Figure 2, the results show that BCT17 has a storage modulus value of 0.2 GPa below 40 °C with a sharp drop to ca. 1 MPa above 40 °C. Although no clear second T_g could be detected, there are minor changes in the DSC trace in this temperature range (Figure S4), indicating that this weakening of the mechanical properties can be attributed to a softening of the hard PBnMA block as it transitions into the rubbery phase. Additionally, these results suggest that there are ordered domains in BCT17 as the mechanical properties of this SPE seem to be determined by the PBnMA block.

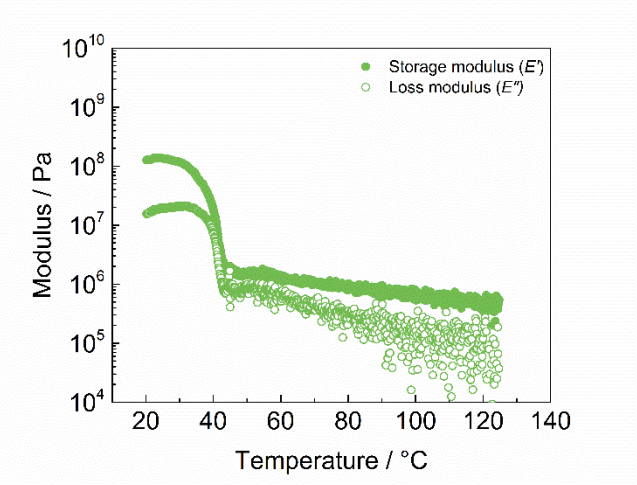

Figure 2. Dynamic mechanical analysis of BCT17 showing its moduli as a function of temperature.

Ion transport. The ionic conductivity of the electrolytes was investigated using electrochemical impedance spectroscopy and the results are presented in Figure 3. Of the investigated electrolytes, BCT17 showed the highest ionic conductivity, which correlates well with the fact that this sample also presented the lowest T_g of the electrolytes (Table 1). The high ionic conductivity for BCT17 is attributed to its optimum free charge carrier concentration and charge carrier mobility. Excessive amounts of salt render a crosslinking effect where coordinated Li^+ ions act as transient bridges between neighboring chains, in addition to ion clustering effects, that together act to reduce polymer and ion mobility.[18, 36] This physical crosslinking is associated with an increasing T_g with salt concentration, as seen in Figure S2. This explains the lower ionic conductivity for electrolytes BCT23 and BCT29 in comparison to BCT17. BCT9 showed the lowest ionic conductivity. At low temperatures, this correlates well with that the sample is semi-crystalline.[18] However, this electrolyte shows markedly lower conductivity also above the melting point (Figure 3), indicating that the lower conductivity is rather a result of a low concentration of free charge carriers.

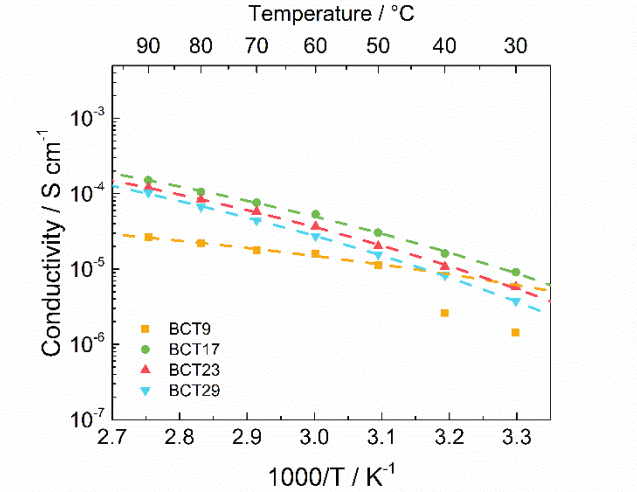

Figure 3. Ionic conductivity as a function of temperature for BCT with 9.1 to 28.6 wt% LiTFSI loadings, calculated from electrochemical impedance spectroscopy. Dashed lines represent VFT fits.

The temperature dependence of the conductivity shows up as curved lines in the Arrhenius plot in Figure 3 for all BCT electrolytes (for BCT9 above T_m). This is typical of ion conduction coupled to segmental motion in amorphous electrolytes above their T_g and is commonly expressed through the empirical Vogel– Fulcher–Tammann (VFT) relationship in Equation (1):

$$\sigma = \sigma_0 T^{-1/2} \exp[-B/(T - T_0)] \qquad (1)$$

where σ_0 is a constant proportional to the number of carrier ions, B is associated with the activation energy, and T_0 is a reference temperature associated with the ideal glass transition temperature at which the configurational entropy becomes zero (often said to be ca. 50 K below T_g).[37] As seen in Figure 3, all electrolytes in this study follow the VFT relationship, indicating that cation movement is coupled to the segmental motions of the polymer.[38] Lithium ions are

coordinated to the carbonyl groups in the polymer chain (the coordination is weaker than for PEO-based electrolytes).[39] Above the T_g, the polymer chains undergo constant local segmental motion and generate free volume, allowing the coordination environment of the lithium ions to change through ligand exchange. The ions may then move through the electrolyte by means of a series of such coordination site transformations.[40] For BCT9, which is semi-crystalline and shows an abrupt change in ionic conductivity at the melting temperature, the VFT relationship applies above T_m. In the case of BCT17, the lack of any kink in the curve at around 40 °C, where a phase transition in the PBnMA block is indicated by both DSC and DMA, indicates that ion conduction predominantly takes place in the PCL–PTMC block. The activation energy of these electrolytes can be calculated from the slope of $\ln(\sigma T^{1/2})$ versus $1/(T-T_0)$ (Figure S5), and the results are given in Table S1. The amorphous SPEs (BCT17, BCT23 and BCT29) featured similar activation energies, between 9.4 and 9.9 kJ mol^{-1}. These values are comparable to the activation energy for the pure conducting block 80:20 PCL–PTMC, indicating that the presence of the mechanical block in the BCT does not entail an additional energy barrier for ion movement. In the case of the semi-crystalline BCT9, the activation energy was calculated above the deflection point (above 50 °C) and is lower than for the higher salt concentrations. The lower activation energy together with the presence of semi-crystallinity for this electrolyte indicates a distinct difference between 9.1 wt% salt and the above concentrations, which could be morphological in origin.

The ionic conductivity of just below 10^{-5} S cm^{-1} at room temperature for BCT17 means that the inclusion of the PBnMA hard block does not incur a sizable penalty to the conductivity compared to an electrolyte prepared from the pure PCL–PTMC copolymer,[19] as illustrated in Figure S6 and is in the same range as those of the gamma-irradiated electrolytes reported by

Mindemark et al.[25] Furthermore, as seen in Figure S6 the ionic conductivity of BCT17 is also superior to that of a PEO:LiTFSI reference electrolyte (20:1 EO:Li^+), particularly below the melting temperature of the semi-crystalline PEO electrolyte. This means that battery devices utilizing PEO-based electrolytes have to be operated above their T_m since the ionic conductivity is significantly lower below 60 °C. The caprolactone-based copolymer electrolytes, on the other hand, are fully amorphous and can therefore be used below 60 °C. An interesting observation is that the BCT electrolyte exhibits its maximum ionic conductivity at 17 wt% LiTFSI (equivalent to 20.9 wt% if only the ion-conducting block is considered), while PEO and the 80:20 PCL–PTMC copolymer require up to 25–28 wt% LiTFSI.

In contrast with PEO-based electrolytes,[41-42] that are characterized by low cation transference numbers (T_+), polycarbonate- and polyester-based SPEs tend to show much higher T_+ values.[19, 21, 23] Using the Bruce–Vincent method,[43] the apparent transference number of the BCT17 electrolyte was determined to be 0.64 ± 0.04 (see data in Table S2), indicating that the majority of the ionic current is carried by the Li^+ cation. This is very close to the value reported for electrolytes prepared from the pure PCL–PTMC copolymer[19] and is well above the usual T_+ of ca. 0.1–0.3 for PEO.[15, 43-44] This confirms that the PBnMA block hardly affects the ion transport properties of the material, which are instead characteristic of the soft PCL–PTMC block.

To further investigate the morphology of these materials, small-angle neutron scattering (SANS) measurements were carried out. Although BCT0 features a small peak that could be related to a phase separation of the material, the addition of LiTFSI does not lead to a clear peak signal which could be correlated to a phase separation in the SPEs (Figure S7). Despite the lack of a clear second T_g in the DSC results and the absence of long-range order confirmed by SANS, the results from the mechanical properties and ionic conductivity indicate that there are indeed

ordered domains in the BCT17 electrolyte that decouple the conductive and mechanical properties of this block copolymer electrolyte.[17] However, it should be noticed that the contrast between the blocks and the added salt is rather low. Thus, it could not be ruled out that the electrolytes are, at least partly, phase separated.

Generally, there is a trade-off between the ionic conductivity and the mechanical properties of a solid polymer electrolyte.[6, 17, 45] One possible way to solve this is by using block copolymers with self-assembled conducting nanostructured blocks and continuous high modulus non-conducting phases, which leads to a decoupling of both properties,[5, 17] There are numerous papers discussing the synthesis, ionic conductivity and morphology of block copolymer electrolytes,[5, 46-48] and recent coupled mechanical-electrochemical simulation work on SPE-based batteries also highlights the importance of the mechanical properties of SPEs in battery systems.[49] Despite this, little effort has been done to experimentally investigate these systematically, and the reported values are usually measured with different techniques or experimental conditions, making the comparison between them very difficult. Nevertheless, a simple comparison would be between BCT17 (9.1×10^{-6} S cm^{-1} and 10^{8} Pa at 30 °C) and the ionic conductivity of 80:20 PCL–PTMC polymer with 28 wt% LiTFSI (2.5×10^{-5} S cm^{-1} at 30 °C) and the mechanical properties of polystyrene (3×10^{8} Pa at 30 °C)[29] (Figure 4). These results suggest, once again, that both properties are decoupled in BCT17. When the PBnMA block is replaced with polystyrene (SCT17), both the ionic conductivity and mechanical properties become inferior,[29] as seen in Figure 4. Besides block copolymers, another way to increase the mechanical properties of an ion conducting polymer is by crosslinking. In this case, BCT17 can be compared to an 80:20 PCL–PTMC crosslinked with gamma irradiation[25] (Figure 4). While the ionic conductivity of both SPEs is similar, the mechanical properties of

BCT17 are clearly superior.[25] BCT17 is thus a highly competitive electrolyte, combining a high modulus with ionic conductivity at low temperatures.

Overall, these results indicate that ionic conductivity and mechanical properties are decoupled in BCT17. Firstly, despite the absence of a clear second T_g for the hard block at around 40 °C, there is a change in mechanical properties at that temperature indicating a phase transition in the polymer electrolyte. This is an indication of decoupled ionic conductivity and mechanical properties. Secondly, although DMA shows a phase transition at 40 °C, the ionic conductivity does not show any abrupt change at that temperature. This indicates that the ion conduction mainly takes place in the PCL–PTMC block and, thus, it is decoupled from the mechanical block. Lastly, the fact that the ionic conductivity of BCT17 is similar to that of 80:20 PCL–PTMC and its storage modulus to polystyrene is further proof that both properties are decoupled.

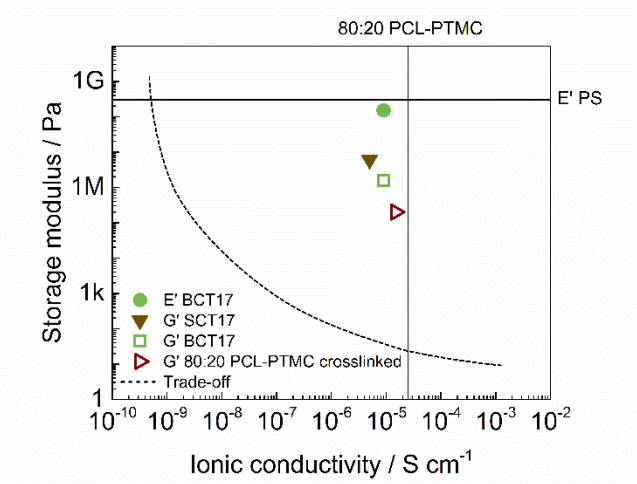

Figure 4. Storage modulus vs ionic conductivity at 30 °C. E' of BCT17 (green circle), E' of SCT17 (brown reverse triangle),[29] G' of BCT17 (green square) at 1 Hz and 25 °C, and G' of 80:20 PCL–PTMC crosslinked with gamma irradiation and 28 wt% LiTFSI at 1 Hz and 25 °C

(red right-pointing triangle).[25] The horizontal line corresponds to the E' value of polystyrene at 30 °C and the vertical line to the ionic conductivity of 80:20 PCL–PTMC with 28 wt% LiTFSI at 30 °C. The dashed line corresponds to the approximate trade-off relationship between lithium ion conductivity and stiffness taken from literature.[45]

Electrochemical performance. In order to determine the potential application of this polymer electrolyte in lithium batteries, stripping/plating tests in symmetric Li │BCT17│Li cells were performed at 0.013 mA cm^{-2} current density and 5 h polarization time at different temperatures (Figure S8) to investigate the stability of the lithium/electrolyte interphase. The cell cycled at 30 °C showed an average polarization of 0.1 V that remained constant during the 70 h experiment. Increasing the temperature to 55 °C resulted in a decrease in overpotential down to 0.03 V and it was maintained for over 250 h. These results show that the BCT17 solid polymer electrolyte has good lithium transport properties, enough to bear the applied current density at ambient and high temperatures for a long time. Additionally, it is electrochemically stable and able to avoid short circuits created by lithium dendrites.

Cyclic voltammetry was performed on the BCT17 electrolyte in a stainless steel *vs.* lithium cell configuration between 5 and −0.5 V (Figure S9) showing good stability at higher but not lower voltages. There is a clear passivation on the first cycle, i.e., the current in the Li plating regime drops, indicating that any decomposition products formed passivate the electrode. However, at ca. 1–2 V on the return scan a relatively high current peak appears and increases over time. The cause of this current peak is not clear, but it may be the result of redox activity by the poly(ε-caprolactone) ester groups.[29]

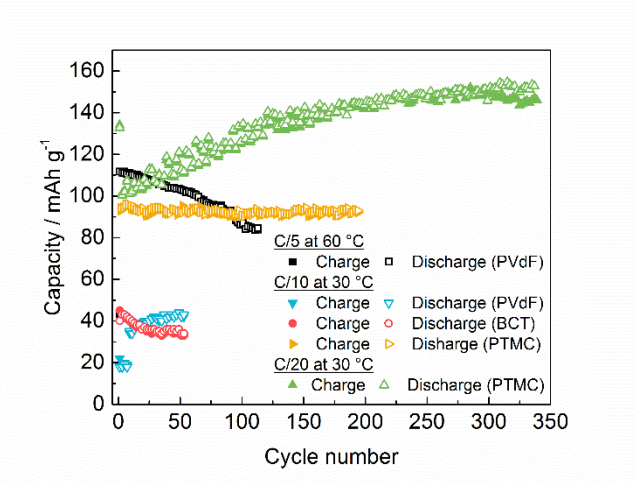

Figure 5. $LiFePO_4$|BCT17|Li half-cells with the cathode binder in parentheses. The capacity decay of the cell cycling at 60 °C at C/5 using PVDF binder (black squares) could be due to an increase in resistance while cycling. The increase in capacity for the cell cycling at 30 °C with PVdF binder (blue reverse triangles) is believed to be due to a bad electrode interface. The second cell cycling at 30 °C is using the BCT17 also as a binder material in the cathode (red circles) to limit mass transport effects. The third cell cycling at 30 °C with PTMC binder (yellow right-pointing triangles) presented higher capacity utilization thanks to a better electrode/electrolyte contact. The capacity is further improved when cycling at 30 °C and C/20 (green triangles).

Having demonstrated fast Li^+ transport, sufficient electrochemical stability and excellent mechanical properties, battery half-cells were prepared by casting a BCT17 electrolyte film directly on top of $LiFePO_4$ cathodes prepared using PVdF as the binder, allowing the electrolyte to infiltrate the porous electrode during preparation in order to maximize the contact between the electrolyte and active material. The cells were allowed to anneal for 6 h at the operating

temperature before cycling, and the open circuit voltage was flat for all cells during this annealing step, indicating that the electrolyte is stable against the cell components. The ion transport properties of the BCT17 electrolyte suggest that cycling of cells prepared using this material should be possible at temperatures close to room temperature, as has recently been shown for several polycarbonate and polyester materials.[19, 50-51] However, as shown in Figure 5, the cell containing PVdF as binder shows an initial low capacity when cycled at 30 °C and C/10, but that increases over time. This phenomenon has previously been observed for cells using PTMC-based electrolytes[20, 24] and is believed to be caused by an electrolyte–electrode interface that develops over time to improve the interfacial ion transfer. Here, this is likely due to the high modulus of the BCT copolymer. When the cycling was done at 60 °C and C/5, the performance was highly improved although the capacity fades constantly from 115 mA h g^{-1} to 80 mA h g^{-1} after 110 cycles. To elucidate the reason for the capacity fade, an intermittent current interruption technique was applied to a BCT17 cell.[35] In this experiment, the resistance was measured from short current interruptions during cycling of the cell to understand how the resistance changes during cycling. As can be seen in Figure 6, the resistance and overpotential increase significantly during cycling. This could be due to the gradual formation of a solid electrolyte interphase (SEI) on the electrodes. However, the resistance reaches a plateau after ca. 50 cycles (Figure S10), indicating that a rather unstable SEI layer is formed at the beginning of the cycling but it stabilizes after 50 cycles. This SEI is formed at a slower rate than that in a liquid electrolyte system where SEI formation is mostly limited to the initial cycle.[52]

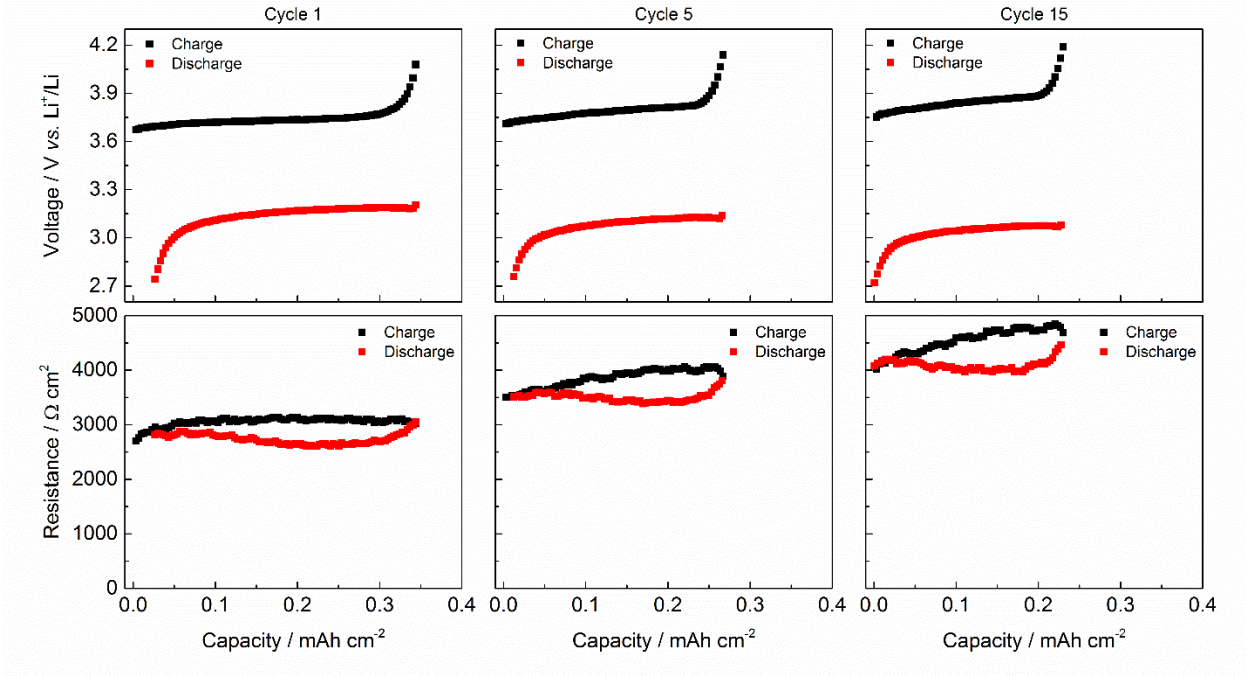

Figure 6. Intermittent current interruption experiment results from a Li|BCT17|$LiFePO_4$ half-cell cycling at 60 °C and at C/10. The cell resistance and polarization increases upon cycling, which may be attributed to limitations in the mass transport between the electrolyte and the active material in the cathode core.

In an attempt to improve the cycling performance at ambient temperatures, a better contact between the electrolyte and the electrode particles is needed. Additional cells were prepared using binders consisting of the polymer electrolytes BCT17 and PTMC containing 17 wt% LiTFSI. Using BCT17 as the binder makes little difference in terms of discharge capacities; at 30 °C and C/10, the cell features an initial discharge capacity of 40 mA h g^{-1} with a small but constant capacity fade upon cycling. This confirms the poor ability of the BCT17

electrolyte to directly form a suitable interface with the $LiFePO_4$ electrode that enables fast Li^+ transfer at this temperature.

In contrast, the cell containing the PTMC electrolyte binder shows much-improved performance; as seen in Figure 5, at 30 °C and C/10 an initial discharge capacity of 94 mA h g^{-1} is reached and maintained for 200 cycles. Furthermore, when the current density is decreased to C/20 the cell containing the PTMC electrolyte binder features an initial discharge capacity of 133 mA h g^{-1}. Although the capacity value decreases in the subsequent cycle, the capacity gradually increases, being fully recovered after 75 cycles, and reaching 151 mA h g^{-1} after 300 cycles. The enhanced electrochemical performance when using PTMC as binder is likely due to a significantly improved electrolyte-electrode interface compatibility. Although it is possible that the PTMC binder also provides a somewhat more beneficial slurry rheology which improves the electrode performance,[53] this is probably not the major cause for the vastly improved cyclability. The macroscopic characters of the electrode slurries are also similar, irrespective of binder used. This highlights the importance of forming an interface between the electrolyte and the electrode that is compatible with the bulk electrolyte in order to facilitate ion transfer over the phase boundary.

CONCLUSIONS

The quest for solid polymer electrolytes with mechanical stability yet high ionic conductivity remains a challenge, but where block copolymers able to decouple these properties constitutes a promising route forward. In this work, an AB block copolymer was synthesized combining 20 wt% of poly(benzyl methacrylate) as the hard block with 80 wt% of poly(ε-caprolactone-*r*-

trimethylene carbonate) as the soft ionic conducting block. The final polymer poly(benzyl methacrylate)-poly(ε-caprolactone-*r*-trimethylene carbonate), abbreviated BCT, was mixed with LiTFSI as the salt. BCT containing 16.7 wt% LiTFSI (BCT17) showed the highest ionic conductivity at ambient temperatures, 10^{-5} S cm^{-1}, and a T_+ of 0.64 calculated using the Bruce–Vincent method. These values are far higher than the values typical of conventional PEO systems, but in line with polycarbonate-based SPEs. The main advantage of BCT, however, is that its mechanical properties are significantly beyond those reported for other block copolymer electrolytes, without compromising the ionic conductivities. This is due to the implementation of a previously little used benzyl methacrylate hard block monomer. DMA analysis revealed that its storage modulus (E') is 0.2 GPa below 40 °C, making this material easy to handle and thus good candidate for, for example, structural all-solid-state batteries. When applying a polycarbonate binder, LFP half-cells delivering 94 and 151 mA h g^{-1} at C/10 and C/20, respectively, at 30 °C could also be constructed.

ASSOCIATED CONTENT

Supporting Information. The following files are available free of charge. NMR spectra, DSC, photos of solid polymer electrolyte while bending, additional ionic conductivity data, data used to calculate the activation energies and apparent transference number, SANS data, symmetric Li │BCT17│Li cycling, cyclic voltammograms, and additional electrochemical results (PDF).

AUTHOR INFORMATION

Corresponding Author

* E-mail: tim.bowden@kemi.uu.se

Present Addresses

† RISE Research Institutes of Sweden, Division Material and production, Isafjordsgatan 28A, Box 7047, 164 40 Kista, Sweden.

Author Contributions

The manuscript was written through contributions of all authors. All authors have given approval to the final version of the manuscript. ‡ These authors contributed equally.

ACKNOWLEDGMENTS

Authors thank the STFC and the ISIS Pulsed Neutron & Muon Source for the provision of neutron beam time, and Dr Stephen King for helping us running the experiments.

REFERENCES

(1) Armand, M.; Tarascon, J. M. Building better batteries. *Nature* **2008,** *451*, 652-657.
(2) Notter, D. A.; Gauch, M.; Widmer, R.; Wager, P.; Stamp, A.; Zah, R.; Althaus, H. J. Contribution of Li-Ion Batteries to the Environmental Impact of Electric Vehicles. *Environ. Sci. Technol.* **2010,** *44*, 6550-6556.
(3) Scrosati, B.; Hassoun, J.; Sun, Y. K. Lithium-ion batteries. A look into the future. *Energy Environ. Sci.* **2011,** *4*, 3287-3295.
(4) Snyder, J. F.; Carter, R. H.; Wetzel, E. D. Electrochemical and mechanical behavior in mechanically robust solid polymer electrolytes for use in multifunctional structural batteries. *Chem. Mater.* **2007,** *19*, 3793-3801.
(5) Young, W.-S.; Kuan, W.-F.; Epps, T. H. Block copolymer electrolytes for rechargeable lithium batteries. *J. Polym. Sci., Part B: Polym. Phys.* **2014,** *52*, 1-16.
(6) Asp, L. E.; Greenhalgh, E. S. Structural power composites. *Compos. Sci. Technol.* **2014,** *101*, 41-61.
(7) González, C.; Vilatela, J. J.; Molina-Aldareguía, J. M.; Lopes, C. S.; Llorca, J. Structural composites for multifunctional applications: Current challenges and future trends. *Prog. Mater Sci.* **2017,** *89*, 194-251.

(8) Wang, Y. Y.; Fan, F.; Agapov, A. L.; Saito, T.; Yang, J.; Yu, X.; Hong, K. L.; Mays, J.; Sokolov, A. P. Examination of the fundamental relation between ionic transport and segmental relaxation in polymer electrolytes. *Polymer* **2014,** *55*, 4067-4076.
(9) Bouchet, R.; Maria, S.; Meziane, R.; Aboulaich, A.; Lienafa, L.; Bonnet, J. P.; Phan, T. N. T.; Bertin, D.; Gigmes, D.; Devaux, D.; Denoyel, R.; Armand, M. Single-ion BAB triblock copolymers as highly efficient electrolytes for lithium-metal batteries. *Nat. Mater.* **2013,** *12*, 452-457.
(10) Ziv, B.; Borgel, V.; Aurbach, D.; Kim, J. H.; Xiao, X. C.; Powell, B. R. Investigation of the Reasons for Capacity Fading in Li-Ion Battery Cells. *J. Electrochem. Soc.* **2014,** *161*, A1672-A1680.
(11) Bergfelt, A.; Rubatat, L.; Mogensen, R.; Brandell, D.; Bowden, T. d_8-poly(methyl methacrylate)-poly (oligo ethylene glycol) methyl ether methacrylate tri-block-copolymer electrolytes: Morphology, conductivity and battery performance. *Polymer* **2017,** *131*, 234-242.
(12) Devaux, D.; Glé, D.; Phan, T. N. T.; Gigmes, D.; Giroud, E.; Deschamps, M.; Denoyel, R.; Bouchet, R. Optimization of Block Copolymer Electrolytes for Lithium Metal Batteries. *Chem. Mater.* **2015,** *27*, 4682-4692.
(13) Ruzette, A.-V. r. G.; Soo, P. P.; Sadoway, D. R.; Mayes, A. M. Melt-Formable Block Copolymer Electrolytes for Lithium Rechargeable Batteries. *J. Electrochem. Soc.* **2001,** *148*, A537.
(14) Thelen, J. L.; Teran, A. A.; Wang, X.; Garetz, B. A.; Nakamura, I.; Wang, Z.-G.; Balsara, N. P. Phase Behavior of a Block Copolymer/Salt Mixture through the Order-to-Disorder Transition. *Macromolecules* **2014,** *47*, 2666-2673.
(15) Timachova, K.; Watanabe, H.; Balsara, N. P. Effect of Molecular Weight and Salt Concentration on Ion Transport and the Transference Number in Polymer Electrolytes. *Macromolecules* **2015,** *48*, 7882-7888.
(16) Yuan, R.; Teran, A. A.; Gurevitch, I.; Mullin, S. A.; Wanakule, N. S.; Balsara, N. P. Ionic Conductivity of Low Molecular Weight Block Copolymer Electrolytes. *Macromolecules* **2013,** *46*, 914-921.
(17) Singh, M.; Odusanya, O.; Wilmes, G. M.; Eitouni, H. B.; Gomez, E. D.; Patel, A. J.; Chen, V. L.; Park, M. J.; Fragouli, P.; Iatrou, H.; Hadjichristidis, N.; Cookson, D.; Balsara, N. P. Effect of Molecular Weight on the Mechanical and Electrical Properties of Block Copolymer Electrolytes. *Macromolecules* **2007,** *40*, 4578-4585.
(18) Mindemark, J.; Lacey, M. J.; Bowden, T.; Brandell, D. Beyond PEO—Alternative host materials for Li^+-conducting solid polymer electrolytes. *Prog. Polym. Sci.* **2018,** *81*, 114-143.
(19) Mindemark, J.; Sun, B.; Törmä, E.; Brandell, D. High-performance solid polymer electrolytes for lithium batteries operational at ambient temperature. *J. Power Sources* **2015,** *298*, 166-170.
(20) Sun, B.; Mindemark, J.; Edström, K.; Brandell, D. Polycarbonate-based solid polymer electrolytes for Li-ion batteries. *Solid State Ionics* **2014,** *262*, 738-742.
(21) Tominaga, Y.; Yamazaki, K. Fast Li-ion conduction in poly(ethylene carbonate)-based electrolytes and composites filled with TiO_2 nanoparticles. *Chem. Commun.* **2014,** *50*, 4448-4450.
(22) Mindemark, J.; Törmä, E.; Sun, B.; Brandell, D. Copolymers of trimethylene carbonate and ε-caprolactone as electrolytes for lithium-ion batteries. *Polymer* **2015,** *63*, 91-98.

(23) Sun, B.; Mindemark, J.; Morozov, E. V.; Costa, L. T.; Bergman, M.; Johansson, P.; Fang, Y.; Furo, I.; Brandell, D. Ion transport in polycarbonate based solid polymer electrolytes: experimental and computational investigations. *Phys. Chem. Chem. Phys.* **2016,** *18*, 9504-9513.
(24) Sun, B.; Mindemark, J.; Edström, K.; Brandell, D. Realization of high performance polycarbonate-based Li polymer batteries. *Electrochem. Commun.* **2015,** *52*, 71-74.
(25) Mindemark, J.; Sobkowiak, A.; Oltean, G.; Brandell, D.; Gustafsson, T. Mechanical Stabilization of Solid Polymer Electrolytes through Gamma Irradiation. *Electrochim. Acta* **2017,** *230*, 189-195.
(26) Monroe, C.; Newman, J. Dendrite growth in lithium/polymer systems - A propagation model for liquid electrolytes under galvanostatic conditions. *J. Electrochem. Soc.* **2003,** *150*, A1377-A1384.
(27) Monroe, C.; Newman, J. The Impact of Elastic Deformation on Deposition Kinetics at Lithium/Polymer Interfaces. *J. Electrochem. Soc.* **2005,** *152*, A396-A404.
(28) Soo, P. P.; Huang, B.; Jang, Y. I.; Chiang, Y. M.; Sadoway, D. R.; Mayes, A. M. Rubbery Block Copolymer Electrolytes for Solid-State Rechargeable Lithium Batteries. *J. Electrochem. Soc.* **1999,** *146*, 32-37.
(29) Bergfelt, A.; Lacey, M. J.; Hedman, J.; Sångeland, C.; Brandell, D.; Bowden, T. ε-Caprolactone-based solid polymer electrolytes for lithium-ion batteries: synthesis, electrochemical characterization and mechanical stabilization by block copolymerization. *RSC Adv.* **2018,** *8*, 16716-16725.
(30) Reiter, J.; Dominko, R.; Nádherná, M.; Jakubec, I. Ion-conducting lithium bis(oxalato)borate-based polymer electrolytes. *J. Power Sources* **2009,** *189*, 133-138.
(31) Zehm, D.; Ratcliffe, L. P. D.; Armes, S. P. Synthesis of Diblock Copolymer Nanoparticles via RAFT Alcoholic Dispersion Polymerization: Effect of Block Copolymer Composition, Molecular Weight, Copolymer Concentration, and Solvent Type on the Final Particle Morphology. *Macromolecules* **2013,** *46*, 128-139.
(32) Bergfelt, A.; Rubatat, L.; Brandell, D.; Bowden, T. Poly(benzyl methacrylate)-poly[(oligo ethylene glycol) methyl ether methacrylate] triblock-copolymers as solid electrolyte for lithium batteries. *Solid State Ionics* **2018,** *321*, 55-61.
(33) Heenan, R. K.; Penfold, J.; King, S. M. SANS at pulsed neutron sources: Present and future prospects. *J. Appl. Crystallogr.* **1997,** *30*, 1140-1147.
(34) Hauffman, G.; Rolland, J.; Bourgeois, J.-P.; Vlad, A.; Gohy, J.-F. Synthesis of nitroxide-containing block copolymers for the formation of organic cathodes. *J. Polym. Sci., Part A: Polym. Chem.* **2013,** *51*, 101-108.
(35) Lacey, M. J. Influence of the Electrolyte on the Internal Resistance of Lithium−Sulfur Batteries Studied with an Intermittent Current Interruption Method. *ChemElectroChem* **2017,** *4*, 1997-2004.
(36) Ratner, M. A.; Shriver, D. F. Ion transport in solvent-free polymers. *Chem. Rev.* **1988,** *88*, 109-124.
(37) Baril, D.; Michot, C.; Armand, M. Electrochemistry of liquids vs. solids: Polymer electrolytes. *Solid State Ionics* **1997,** *94*, 35-47.
(38) Agrawal, R. C.; Pandey, G. P. Solid polymer electrolytes: materials designing and all-solid-state battery applications: an overview. *J. Phys. D: Appl. Phys.* **2008,** *41*, 223001.
(39) Mindemark, J.; Lacey, M. J.; Bowden, T.; Brandell, D. Beyond PEO—Alternative host materials for Li^+-conducting solid polymer electrolytes. *Prog. Polym. Sci.* **2018**, DOI: 10.1016/j.progpolymsci.2017.12.004.

(40) Gray, F. M., Polymer electrolytes II: Physical principles. In *Solid State Electrochemistry*, Bruce, P. G., Ed. Cambridge University Press: Cambridge, 1994; pp 119-162.
(41) Buriez, O.; Han, Y. B.; Hou, J.; Kerr, J. B.; Qiao, J.; Sloop, S. E.; Tian, M.; Wang, S. Performance limitations of polymer electrolytes based on ethylene oxide polymers. *J. Power Sources* **2000,** *89*, 149-155.
(42) Pesko, D. M.; Timachova, K.; Bhattacharya, R.; Smith, M. C.; Villaluenga, I.; Newman, J.; Balsara, N. P. Negative Transference Numbers in Poly(ethylene oxide)-Based Electrolytes. *J. Electrochem. Soc.* **2017,** *164*, E3569-E3575.
(43) Evans, J.; Vincent, C. A.; Bruce, P. G. Electrochemical measurement of transference numbers in polymer electrolytes. *Polymer* **1987,** *28*, 2324-2328.
(44) Chintapalli, M.; Timachova, K.; Olson, K. R.; Mecham, S. J.; Devaux, D.; DeSimone, J. M.; Balsara, N. P. Relationship between Conductivity, Ion Diffusion, and Transference Number in Perfluoropolyether Electrolytes. *Macromolecules* **2016,** *49*, 3508-3515.
(45) Asp, L. E. Multifunctional composite materials for energy storage in structural load paths. *Plastics, Rubber and Composites* **2013,** *42*, 144-149.
(46) Meabe, L.; Lago, N.; Rubatat, L.; Li, C.; Müller, A. J.; Sardon, H.; Armand, M.; Mecerreyes, D. Polycondensation as a Versatile Synthetic Route to Aliphatic Polycarbonates for Solid Polymer Electrolytes. *Electrochim. Acta* **2017,** *237*, 259-266.
(47) Niitani, T.; Shimada, M.; Kawamura, K.; Dokko, K.; Rho, Y.-H.; Kanamura, K. Synthesis of Li^+ Ion Conductive PEO-PSt Block Copolymer Electrolyte with Microphase Separation Structure. **2005,** *8*, A385-A388.
(48) Thelen, J. L.; Wang, A. A.; Chen, X. C.; Jiang, X.; Schaible, E.; Balsara, N. P. Correlations between Salt-Induced Crystallization, Morphology, Segmental Dynamics, and Conductivity in Amorphous Block Copolymer Electrolytes. *Macromolecules* **2018,** *51*, 1733-1740.
(49) Grazioli, D.; Verners, O.; Zadin, V.; Brandell, D.; Simone, A. Electrochemical-mechanical modeling of solid polymer electrolytes: Impact of mechanical stresses on Li-ion battery performance. *Electrochim. Acta* **2019,** *296*, 1122-1141.
(50) He, W.; Cui, Z.; Liu, X.; Cui, Y.; Chai, J.; Zhou, X.; Liu, Z.; Cui, G. Carbonate-linked poly(ethylene oxide) polymer electrolytes towards high performance solid state lithium batteries. *Electrochim. Acta* **2017,** *225*, 151-159.
(51) Kimura, K.; Yajima, M.; Tominaga, Y. A highly-concentrated poly(ethylene carbonate)-based electrolyte for all-solid-state Li battery working at room temperature. *Electrochem. Commun.* **2016,** *66*, 46-48.
(52) Verma, P.; Maire, P.; Novák, P. A review of the features and analyses of the solid electrolyte interphase in Li-ion batteries. *Electrochim. Acta* **2010,** *55*, 6332-6341.
(53) Jeschull, F.; Brandell, D.; Wohlfahrt-Mehrens, M.; Memm, M. Water-Soluble Binders for Lithium-Ion Battery Graphite Electrodes: Slurry Rheology, Coating Adhesion, and Electrochemical Performance. *Energy Technol.* **2017,** *5*, 2108-2118.